

PLASMA HEATING BY NEUTRAL BEAM INJECTION

R. Koch

Laboratory for Plasma Physics
Ecole Royale Militaire - Koninklijke Militaire School
B-1000 Brussels , Belgium

ABSTRACT

The additional heating of plasmas by injection of fast neutrals – or Neutral Beam Injection (NBI) - is reviewed. First, the limitations of ohmic heating in tokamaks and the other motivations for using additional heating in fusion machines are discussed. Next, the principle of operation of neutral beam injectors, and state of the art, are outlined. Positive-ion (PNBI) and negative-ion (NNBI) based concepts are discussed. Next, the physical processes by which the beam transfers energy to the plasma, namely ionisation and slowing-down are described. For both, an elementary theory is given and the comparison with experimental results is made. Applications of NBI to heating, current drive and rotation drive are reviewed. The prospects of NBI for ITER are commented.

I. INTRODUCTION

The plasma of a tokamak cannot be heated to ignition using ohmic heating only because the Joule heating efficiency decreases with the plasma temperature and because the maximum value of the plasma current is limited by the onset of magnetohydrodynamic instabilities that kill the discharge (disruption). These limitations of ohmic heating will be briefly discussed in the next section. This is the first reason why auxiliary heating systems are required in tokamaks. For steady-state tokamak operation, also the plasma current needs to be sustained by external means, because the inductive current generation is by essence a non-stationary phenomenon. Because the momentum transfer required to generate a current is necessarily accompanied by energy transfer, any non-inductive current-drive method is also a heating method. Specific current-drive aspects will be treated in a subsequent lecture in these proceedings¹. In other fusion reactor concepts like stellarators, the plasma must be both created and heated by external means. Therefore in all these cases, additional heating systems are required. They can also be used for the production of plasma for wall cleaning and conditioning, ramping-up of the plasma

current at the beginning of the discharge, tailoring of the plasma current profile in the stationary current phase, inducing toroidal rotation. Some more exotic applications are: inducing a poloidal rotation, influencing fast particle transport or stabilising MHD modes. The methods allowing doing this are termed "additional heating" methods, although in some cases they constitute in fact the primary or only source of plasma heating.

There are basically two ways of increasing the energy content of the plasma: one can inject either highly energetic particles or electromagnetic energy inside the plasma. In both cases the energy must eventually be transferred to the bulk of the plasma and, ultimately to the fuel-ion component to generate the fusion reactions. The thermalization of the externally injected energy usually takes place through collisional processes: the injected fast particle or the particle accelerated by the electromagnetic field transfers its energy to the plasma background by collisions.

II. LIMITATIONS OF OHMIC HEATING

The power dissipated by the current flowing in a tokamak plasma is called "Ohmic Heating" power or "OH" power. It could also be called "Joule heating" as it is due to the dissipation associated with the electrical resistance of the plasma. The plasma current is an electron current and the resistivity is due to the collisions of the conduction electrons with the -essentially immobile- background ions. The resistance of the plasma loop is

$$R_p = \frac{10^{-3} R_0 Z_{eff}}{a^2 \kappa \gamma_E(Z_{eff})} \left[1 + \sqrt{\frac{a}{R_0}} \right] T_{e,av}^{-3/2} \quad (1)$$

where R_0 and a are the plasma major and minor radii, κ is the elongation, Z_{eff} is the effective ion charge, γ_E is a function of Z_{eff} that can be approximated by

$$\gamma_E(Z_{eff}) = 1 - 0.98 / Z_{eff} + 0.56 / Z_{eff}^2 \quad (2)$$

Note that this function takes a value close to 1/2 for clean plasmas. In Eq.(1), the factor in square brackets accounts for the trapped particle corrections, and $T_{e,av}$ is some

volume-averaged electron temperature expressed in eV's. [Unless explicitly stated otherwise, like above for temperatures, SI units are used throughout the paper.] The $T^{-3/2}$ dependence reflects the fact that the strength of the collisions decreases as the cube of the relative velocity between the colliding species. This dependence also implies that the plasma resistance quickly drops as the plasma becomes hotter. The ohmic power is also proportional to the square of the plasma current (I_p):

$$P_{OH} = R_p I_p^2 \quad (3)$$

So, although the resistance falls down when the current is increased, as a result of the plasma heating, it is not clear from Eqs (1-3) whether the ohmic power increases or decreases with current. In order to investigate further the consequences of the fall in resistivity, we need a relation linking T_e to I_p .

This is available from the so-called scaling laws for tokamaks² that provide an expression for the total energy content of the plasma W as a function of the various plasma parameters. In the ohmic regime, the so-called ITER89 scaling is:

$$W_{OH} = 64 \times 10^3 M^{0.2} (10^{-6} I_p)^{0.8} R_0^{1.6} a^{0.6} \kappa^{0.5} (10^{-20} n)^{0.6} B_T^{0.35} \quad (4.1)$$

where the new parameters introduced are the isotopic mass M , and the line-averaged density n . Equating this expression to the definition of the total plasma energy content (k_B is Boltzmann's constant)

$$W_{OH} = \pi a^2 2\pi R_0 3n k_B T_{av} \quad (4.2)$$

we get

$$T_{av} = 68 M^{0.2} (10^{-6} I_p)^{0.8} R_0^{0.6} a^{-1.4} \kappa^{-0.5} (10^{-20} n)^{-0.4} B_T^{0.35} \quad (5)$$

where T_{av} is in eV. It is amazing to note that because

$$T_{av} \propto I_p^{0.8} \quad (6)$$

$\tau_E = W_{OH}/P_{OH}$ is independent of the current, i.e. the energy confinement time is independent of the heating power. This situation, which is characteristic of the "good" ohmic confinement, is in strong contrast with the confinement degradation observed in auxiliary heated discharges where

$$\tau_E \propto P_{tot}^{-0.5} \quad (7)$$

However good the ohmic confinement, ohmic heating nevertheless is insufficient to bring a large machine to ignition. Using ITER-FDR-type parameters ($R_0=7.75$ m, $a=2.8$ m, $\kappa=1.6$, $I_p=25$ MA, $B_T=6$ T), Eq.(5) implies $T_{av} \approx 1.3$ keV. Even taking into account that the temperature profile is peaked, this means that it is going to be very difficult to get in OH a central temperature in excess of 3-4 keV.

Why not increase the current above 25MA? Because one then encounters the q -limit, discussed earlier in these proceedings³, above which the plasma becomes

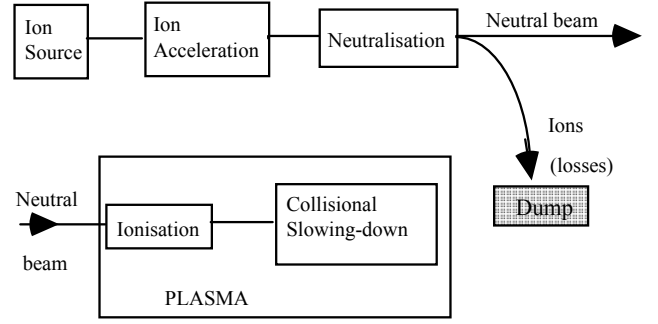


Fig. 1. Sketch of the principle of neutral beam heating. On top, generation of the neutral beam in the injector. Bottom, capture of the neutral beam energy in the plasma.

magnetohydrodynamically unstable and disrupts. This condition ($q_d > 2$) can be written

$$I_p [\text{MA}] = \frac{5a^2 \kappa}{2R_0} B_T \quad (8)$$

which means that 25MA is about the maximum current that can be obtained in a machine of this size. Therefore additional heating is required to bridge the gap to ignition. These conclusions, resting here on very simple considerations, are corroborated by more sophisticated simulations⁴.

III. NEUTRAL BEAM INJECTION

Because of the strong toroidal magnetic field, there is no possibility to directly inject energetic *charged* particles inside the plasma. Instead, one injects fast neutrals at the expense of going through the sequence schematically described in Fig.1. The ions are produced in the source and accelerated to a high energy, usually electrostatically, before crossing a charge exchange cell where they are neutralised. The neutralisation is only partial and the remaining ions are deflected magnetically and sent to a dump. Usually, their energy is lost but it is conceivable to recover it by biasing the dump. The neutrals can then cross the machine's magnetic field and

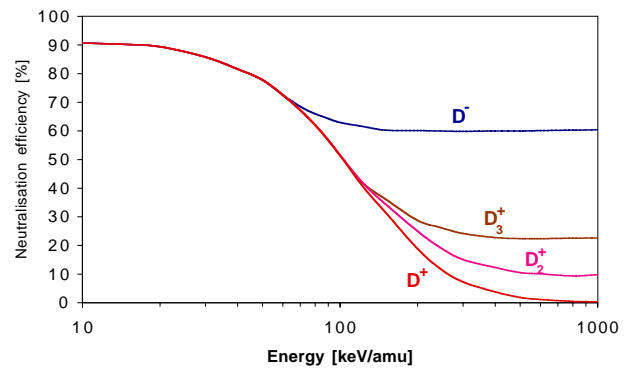


Fig. 2. Maximum neutralisation efficiency of atomic and molecular ions following Berkner et al.⁵

reach the plasma where they get ionised, transferring afterwards their energy to the plasma bulk by collisions. The beam source is a plasma discharge from which the ions are extracted by an electrostatic potential. A hydrogenic plasma discharge –for example in deuterium– not only produces atomic ions, D^+ and D^- , but also molecular ions D_2^+ , D_3^+ . After acceleration at high energy, these ions are neutralised with very different efficiencies. Figure 2 shows that the maximum neutralisation efficiency of a gas cell becomes very small for an atomic D^+ ion above some 200 keV. This is why high energy beam injectors are based on negative ion technology. At lower energy, it is more appropriate to use positive-ion based injectors as the production of positive ions is much easier than that of negative ions.

III.A. Neutral beam injectors (based on positive ions)

All present-day injectors, except one discussed in next section, are based on positive ion (H^+, D^+, \dots) technology. There exists nowadays neutral beam injectors able to deliver 1-2MW of neutrals at energies up to 150 keV. We shall now briefly describe some characteristic features of these injectors. As noted above, the plasma source generates various ion species. After extraction by a negative potential, the negative ions are eliminated but the molecular ions (D_2^+, D_3^+, \dots) remain present in the beam. After acceleration, all ions have the same energy, say E_0 but, as molecular ions contain several atoms, the final beam of neutrals delivered to the plasma will provide after dissociation of molecules and ionisation, in addition to the full energy (atomic) beam ions at E_0 energy, ions at energy $E_0/2$ and $E_0/3$. Some 30% of the total beam power can be carried by these less energetic components that deposit their energy more at the outside of the plasma, as compared to the full energy component. This is a feature that has to be taken into account for computing power deposition profiles. When crossing the neutralisation cell, each ion has a neutralisation probability that first increases with the length of its path in the cell. Afterwards, neutralised ions can be re-ionised again and the neutralisation efficiency decreases⁵. Each ion thus has a maximum neutralisation probability for a given thickness of the cell, different for each type of ion. Figure 2 shows this maximum neutralisation efficiency. It indicates that for beams with energy below 150 keV, the molecular composition of the beam is that of the source. It also points to the limited efficiency of positive-ion based injectors, which falls below 50% around 100 keV.

The energy that can be reached –at reasonable efficiency– with positive-ion based technology is insufficient for the next generation of machines. For the *heating* of the ITER plasma 0.5MeV beams are required. If the beams are to be used to non-inductively *generate*

the plasma *current*, energies of 1-2MeV are required. This is clearly out of reach of any positive-ion based neutral beam and efforts are presently devoted to the development of neutral beams based on a negative-ion source.

III.B. Negative-ion based injectors

In their principle, negative-ion beam injectors are identical to the positive-ion based ones, as sketched in Fig.1. The differences are that (i) The source must preferentially produce negative ions, (ii) Negative-ion based beams operate at much higher energy (0.5 - 2 MeV). The electron captured in the negative ion has a very low binding energy –called affinity– of 0.75 eV. It is therefore very easy to loose, and this feature explains why a high neutralisation efficiency can be achieved with negative ions (Fig.2). The reverse side of the medal is that these ions are hard to produce. In order to increase their rate of production, one incorporates caesium in the source, an element which has very low ionisation potential ($E_I=3.894$ eV), and which therefore easily liberates electrons. Two production mechanisms are exploited: surface and volume production. In *surface production* the ions are produced when atoms bounce off walls coated with caesium. As intense wall bombardment is required to get a large negative ion yield, high power densities are required and the initial energy of the negative ions is rather large. Hence the difficulty to operate these sources for long pulses and to produce well focalised ion beams. *Volume production* rests on a process called “dissociative attachment” whereby a hydrogen molecule in a high vibrational state breaks up at the time it captures an electron. The efficiency of this mechanism was experimentally found to be unexpectedly large. Nevertheless, the ion yield seems to be severely limited, the high gas pressure required leads to early dissociation of the negative ions and a high stray electron current (10 to 100 times the negative ion current) is produced. The presently most efficient sources sort of combine both mechanisms through caesium seeding of volume sources. This increases the negative ion yield, minimises the stray electron current (now 1-5 times the negative ion current only) and reduces the isotopic effect. (The production of D^- is only about half that of H^- in volume sources. This is raised to 80% in Cs seeded sources).

Negative ion sources are equipped with extractors that suppress the stray electron current by superposing the field of permanent magnets to the extracting electrostatic field. The stray electrons hit the extractor grid while the negative ion trajectories are nearly unaffected. These ions are then accelerated electrostatically up to energies of the order of the MeV and neutralised. Two types of accelerators are presently under development. The

MAMuG (for Multi-Aperture Multi-Gap) accelerates in parallel a number of beamlets in steps of typically 200 keV. On the contrary, the SINGAP combines all beamlets into one single broad beam and provides the acceleration over a single gap. Like for positive ion beams, the simplest neutralisation cell is a box filled with gas. At high energy, the maximum efficiency of such a gas neutraliser is about 60% (Fig.2). The adverse mechanism is re-ionisation of fast neutrals (D^+ , H^+ produced). Theoretically, plasma neutralisers could reach an efficiency of up to 85% if the plasma in the cell is fully ionised. (The efficiency decreases if the plasma is only partially ionised). However the realisation of a reliable cell with fully ionised plasma is much more delicate than the gas cell technology.

The target of negative-ion based beam technology is to develop D^0 injectors with, typically, an energy of 1 MeV and a current of 40A in order to couple 50MW in ITER with three units. The best results have been achieved with the JT-60U injector. This injector was designed for pulses of 10MW for 10s at 0.5MeV⁶. The highest parameters reached up to now with this injector are⁷: 400 keV, 5.2 MW, pulse duration 1.9s, for D injection. The neutralisation efficiency of 60% has been achieved, in agreement with predictions. More details about the physics of negative-ion beams can be found in the review paper by Paméla⁸.

III.C. Penetration, ionisation, losses

Neutral beams are usually injected close to the plasma equatorial plane as this provides in front of the beam the longest path through the densest part of the plasma. With respect to the toroidal direction, beams are usually injected either nearly parallel or nearly perpendicular. This last solution is technologically easiest but the path through the plasma is rather small and the fast ions are created with large perpendicular energies and therefore a substantial fraction of them can be immediately trapped into banana orbits (see Fig.3). This

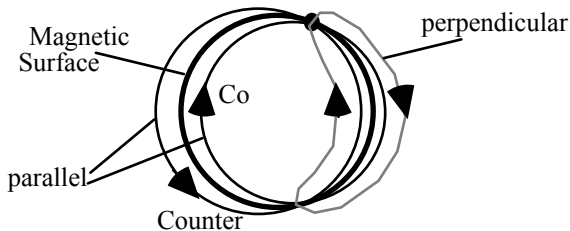


Fig. 3. Poloidal projection of the drift trajectories of beam ions for perpendicular injection (trapped trajectory) and for parallel co- and counter-injection.

can lead to significantly larger prompt ion-loss than in the case of parallel injection. Parallel injection beam lines are harder to design because of the limited amount of space available in between the toroidal field coils. However they provide a much larger path for the ionisation of the beam and most of the ions are created along passing trajectories. In the parallel injection case, neutrals can be injected in the same direction as the plasma current (co-injection) or in the opposite direction (counter-injection). Due to the asymmetry created by the poloidal field, these two parallel injection schemes are not equivalent. As shown in Fig.3 the orbits of the counter-injected ions drift further outside the magnetic surface on which they were injected than the co-injected ions. This leads to a somewhat broader power deposition profile in the counter-injection case.

There are two main sorts of losses involved in the energy transfer from the neutral beam to the plasma. (i) Some neutrals cross the plasma without being ionised and are lost on the wall opposite to the injection point. These are called *shinethrough* losses. (ii) Fast ions can get neutralised shortly after their ionisation. The so created neutrals will either leave the plasma or be re-ionised at an arbitrary radius. This leads to direct losses and broadening of the power deposition profile. Because the neutralisation process is mainly due to charge-exchange (see below), the corresponding losses are called *charge-exchange* (CX) losses. In the analysis of beam-heated discharges, these losses are usually subtracted from the injected beam power to yield the net power delivered to the plasma taken into account in confinement (power-balance) evaluations. Other losses can occur, especially for non-parallel injection, due to superbanana losses, i.e. loss of banana particles trapped in the ripples of the toroidal magnetic field. Finally if the ions are injected at a velocity faster than the local Alfvén velocity, they can excite global modes –the toroidal Alfvén eigenmodes (TAE)- and be ejected out of the plasma by interaction with the TAE's electromagnetic fields.

The ionisation of the beam is due to several processes: ionisation by impact on electrons and ions (both hydrogenic and impurities), charge exchange and multistep ionisation. The dominant process for the lower energy range (e.g. $W_{b0} \leq 80$ keV for deuterons) is charge exchange. The cross-section for charge-exchange with protons was given by Riviere⁹ (with $E = W_{b0}/M_b$, in eV/amu, W_{b0} is the energy of the beam neutral and M_b its isotopic mass number)

$$\sigma_{CX} = 0.6937 \times 10^{-18} \frac{(1 - 0.155 \log_{10} E)^2}{1 + 0.1112 \times 10^{-14} E^{3.3}} \quad (9)$$

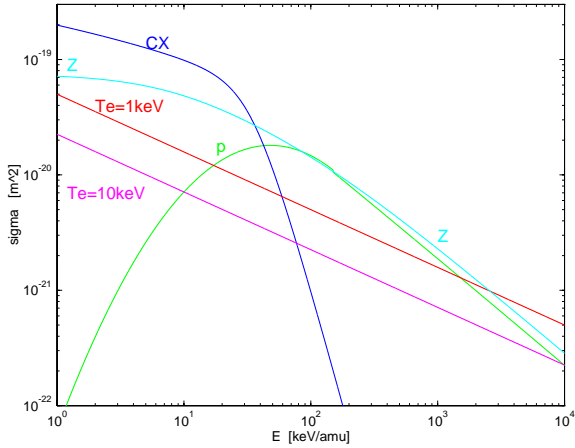


Fig. 4. Cross sections for ionisation of fast neutrals by charge-exchange (CX), electron impact (for two different electron temperatures $T_e=1$ and 10 keV), and by proton impact (p). The curve Z is the normalised $\tilde{\sigma}_Z(E)$ for impurities.

At higher energy, proton and electron impact ionisation become dominant. The cross-section for proton impact is⁹

$$\log_{10} \sigma_p = -0.8712(\log_{10} E)^2 + 8.156 \log_{10} E - 38.833 \quad \text{for } E < 150 \text{ keV} \quad (10.1)$$

$$\sigma_p = 3.6 \times 10^{-16} \log_{10}(0.1666 E) / E \quad \text{else} \quad (10.2)$$

and for electron impact¹⁰

$$\bar{\sigma}_e = \frac{\langle \sigma_e v_e \rangle}{v_{b0}} \quad (11)$$

where

$$v_{b0} = 1.3715 \times 10^4 \sqrt{E} \quad (12)$$

is the velocity of the neutral and $\langle \sigma_e v_e \rangle$ is the ionisation rate averaged over the electron distribution and is a function of the electron temperature T_e only. These three cross-sections are represented in Fig.4. If the plasma contains impurities, these can cause additional ionisation. The cross-section σ_Z for ionisation by impurities with atomic number Z can be written¹¹ in terms of a scaled-to-charge cross-section $\tilde{\sigma}_Z$:

$$\sigma_Z = Z \tilde{\sigma}_Z(E / Z) \quad (13.1)$$

$$\tilde{\sigma}_Z(w) = 7.457 \times 10^{-20} \left[\frac{1}{1 + 0.08095 w} + \frac{2.754 \ln(1 + 1.27 w)}{64.58 + w} \right] \quad (13.2)$$

The scaled cross-section $\tilde{\sigma}_Z$ is also represented in Fig.4. In total, the ionisation rate per unit length will be, in the example of an H plasma with a single impurity:

$$-\frac{1}{I_b} \frac{dI_b}{dl} = n_e \sigma_e + n_H \sigma_p + n_H \sigma_{CX} + n_Z \sigma_Z \quad (14)$$

where we have denoted by I_b the beam intensity and dl the elementary path length along the neutral's trajectory. We define the total or *beam-stopping* cross-section as:

$$\sigma_0 = \sigma_e + \frac{n_H}{n_e} (\sigma_p + \sigma_{CX}) + \frac{n_Z}{n_e} \sigma_Z \approx \sigma_e + \sigma_p + \sigma_{CX} + \frac{n_Z}{n_e} \sigma_Z \quad (15)$$

Note, in particular, that the effect of the impurities is proportional to their concentration. This cross-section was deemed satisfactory for the range of energies typical of early PNBI injection in not too dense plasmas ($n_e \approx 10^{19} \text{ m}^{-3}$, $E \approx 30\text{-}40 \text{ keV}$). However, when the injection energy becomes larger, which is typically the case with NNBI, and/or for larger densities, this formula underestimates the cross-section because it ignores *multi-step ionisation*. This is the process by which a neutral first gets into excited states due to successive collisions before being ionised. This process is negligible for a (relatively) slow neutral in a low density plasma because the lifetime in the excited state is much shorter than the time between two successive collisions. If the speed of the neutral or the number of particles per unit volume increases sufficiently, this is no longer the case. Multi-step ionisation can be taken into account by introducing the *beam stopping increment* δ_{ms} into the complete cross-section σ

$$\sigma = \sigma_0 (1 + \delta_{ms}) \quad (16)$$

The complete cross-sections have been computed by Janev et al.¹¹, and more recently by Suzuki et al.¹². These authors also provide analytic fits to the data. The correction due to multi-step ionisation can go to 100% or more for NNBI¹³. For PNBI, the correction is usually less than 20%.

The mean-free path of the neutrals in a plasma of density n is

$$\lambda = \frac{1}{n \sigma} \quad (17.1)$$

and the evolution of the neutral beam intensity $I_b(l)$ (for a narrow beam) follows from Eq.(14):

$$I_b(l) = I_{b0} \exp \left\{ - \int_0^l \sigma(\mathbf{r}) n(\mathbf{r}) dl \right\} \quad (17.2)$$

where the integration is along the path $\mathbf{r}(t)$ of the neutral in the plasma.

Once created, the ion will follow a trapped or passing orbit, as already discussed. If the confinement of fast particles in the machine is sufficiently good, the ion can be assumed to stay on its magnetic surface and to slow down there by collisions. In a first approximation it is thus sufficient to study the slowing-down process as if it was taking place in an infinite homogeneous plasma having the same parameters as those of the magnetic surface. Neo-classical effects can be taken into account by the so-called bounce-averaging¹⁴ procedure over the real drift-trajectories of particles but this topic will be left out in the present elementary presentation.

We shall now investigate the slowing-down process in the homogeneous plasma limit. This can be examined through two complementary approaches: the test-particle

and the Fokker-Planck ones. The latter allows computing the fast-ion distribution function.

III.D. Slowing down. Test-particle approach

Starting from the theory of binary Coulomb collisions Sivukhin¹⁵ has shown that the energy decrease of a particle due to the background species s with maxwellian distribution

$$f_s(v) = \frac{1}{(\sqrt{2\pi}V_{ts})^3} \exp\left[-\frac{v^2}{2V_{ts}^2}\right] \quad (18.1)$$

and thermal velocity $V_{ts} = \sqrt{k_B T_s / m_s}$ is:

$$\frac{dW_b}{dt} = -\frac{4\pi Z_b^2 e^2}{v_b} \sum_s (\ln \Lambda) n_s Z_s^2 e^2 \times \left[\frac{\text{Erf}(w_s)}{m_s} - \frac{2w_s(m_s + m_b)}{m_s m_b \sqrt{\pi}} e^{-w_s^2} \right] \quad (18.2)$$

with $w_s = v_b / \sqrt{2} V_{ts}$ and the index “b” refers to the beam ions.

Consider a background plasma with ions ($s=i$) and electrons ($s=e$). For a 5keV plasma, for example, the thermal electron velocity V_{te} is in the range of $3 \cdot 10^7$ m/s while $V_{ti} = 5 \cdot 10^5$ m/s. A 100 keV ion has a velocity of $3 \cdot 10^6$ m/s. Therefore it is usually justified to make the assumption that the injected ions are much slower than the average electron ($w_e \ll 1$) and much faster than the average ion ($w_i \gg 1$). This simplifies considerably Eq.(18.2) as $\text{Erf}(x) \approx 2x / \sqrt{\pi}$ for $x \ll 1$ and $\text{Erf}(x) \approx 1$ for $x \gg 1$ and Eq.(18) can be written

$$\frac{dW_b}{dt} = -\frac{2W_b}{\tau_s} \left[1 + \left(\frac{W_e}{W_b} \right)^{3/2} \right] \quad (19)$$

where the first term in the square brackets corresponds to energy transfer to the electrons and the second one to the

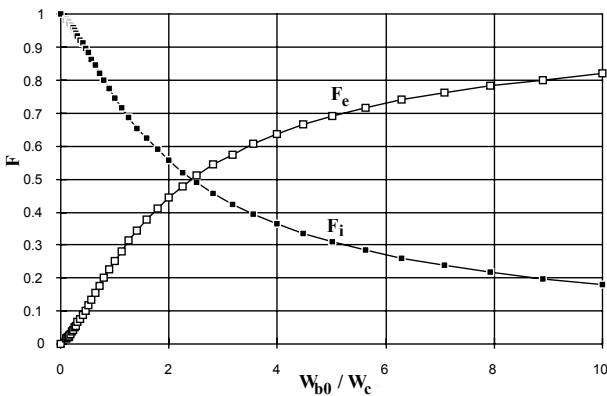


Fig.5. Fractions F_e and F_i of the beam ions energy going respectively to electrons and to ions during the slowing down process.

background ions. When $W_c = W_b$ an equal amount of power is transferred to electrons and ions. W_c is called the critical energy and has the value

$$W_c = \frac{1}{2} m_b v_c^2 = 14.8 T_e [\text{keV}] M_b \left(\frac{1}{n_e} \sum_i \frac{n_i Z_i^2}{M_i} \right)^{2/3} \quad (20)$$

The critical velocity is

$$v_c = \sqrt{\frac{2k_B T_e}{m_e}} \left(\frac{3\sqrt{\pi}}{4} \sum_i \frac{n_i}{n_e} Z_i^2 \frac{m_e}{m_i} \right)^{1/3} \quad (21)$$

When the beam ion velocity is much larger than the critical velocity ($W_b \gg W_c$), Eq.(19) becomes much simpler

$$\frac{dW_b}{dt} = -\frac{2}{\tau_s} W_b \quad (22)$$

and describes a simple exponential decay. In this case all the energy is transferred to the electrons. Note that for the α -particles ($M_\alpha=4$, $Z_\alpha=2$, $W_{\alpha 0}=3.5$ MeV) generated in a thermonuclear plasma ($T_e \approx 10$ keV) one has

$$\left(W_c / W_\alpha \right)^{3/2} \approx 10^{-2} \quad (23)$$

implying that α -particles, in a reactor, will heat the electrons rather than the ions. In the case of dominant electron slowing-down the characteristic energy decay time is $\tau_s/2$. τ_s is called the (electron) slowing-down time and is given by the expression

$$\tau_s = \frac{3(2\pi)^{3/2} m_e m_b e_0^2 V_{te}^3}{n_e Z_b^2 e^4 \ln \Lambda} \approx 0.012 \frac{(T_e [\text{keV}])^{3/2} M_b}{n_e [10^{20} \text{ m}^{-3}] Z_b^2} \quad (24)$$

(with $\ln \Lambda = 16.5$). For a 40keV deuteron in a 1keV, $5 \cdot 10^{19} \text{ m}^{-3}$ TEXTOR plasma, this gives $\tau_s \approx 50$ ms. For an α -particle in a 10keV, 10^{20} m^{-3} plasma $\tau_s \approx 400$ ms. At this point it should be noted that these values are not far from the energy confinement time values. Therefore, transport can play a role on the same time-scale as slowing-down in the process of energy transfer from the beam to the plasma (or from the α -particle in a reactor plasma).

The above Eqs.(19,22) describe the instantaneous slowing down of an ion in the plasma. Two other important quantities that describe the whole slowing-down process, from birth velocity to thermal velocity, are the fraction of the total energy that has gone to electrons (F_e) and to the ions (F_i) after complete slowing-down. This is easily evaluated from Eq.(19). The instantaneous power transferred to the ions is:

$$P_i = \frac{2W_b}{\tau_s} \left(\frac{W_e}{W_b} \right)^{3/2} \quad (25)$$

and the energy transferred to the ions during the whole slowing-down process is

$$W_i = \int_0^\infty P_i dt \quad (26)$$

Noting that one can re-write Eq.(19) as

$$-\frac{2}{\tau_s} dt = \frac{dy}{y(1+y^{-3/2})}; \quad y = W_b / W_c \quad (27)$$

we get for $F_i = W_i/W_{b0}$ where W_{b0} is the beam energy

$$F_i = \frac{-1}{W_{b0}} \int_0^\infty W_b \left(\frac{W_c}{W_b} \right)^{3/2} \left(-\frac{2}{\tau_s} \right) dt = \frac{W_c}{W_{b0}} \int_0^{W_{b0}/W_c} \frac{dy}{1+y^{3/2}} \quad (28)$$

$$\text{and } F_e = 1 - F_i \quad (29)$$

A plot of these fractions is given in Fig.5.

III.E. Slowing down. The beam distribution function.

The starting point of a computation of the distribution function is the Fokker-Planck equation. Its derivation can be found in Sivukhin¹⁵. This equation can be written:

$$\frac{df_b}{dt} = \sum_s C(f_b, f_s) + C(f_b, f_b) + S + L \quad (30)$$

where $C(f_b, f_s)$ is the collision integral for particles of type b and s . The first sum is over all the background plasma species and the 2nd term accounts for collisions among the beam particles themselves. Usually one uses as starting point the Landau form of the collision integral¹⁶:

$$C(f_b, f_s) = \frac{Z_b^2 Z_s^2 e^4 \ln \Lambda_{bs}}{8\pi\epsilon_0^2 m_b} \frac{\partial}{\partial \mathbf{v}} \cdot \int \frac{u^2 \mathbf{I} - \mathbf{u}\mathbf{u}}{u^3} \times \left[\frac{f_s(\mathbf{w})}{m_b} \frac{\partial f_b(\mathbf{v})}{\partial \mathbf{v}} - \frac{f_b(\mathbf{v})}{m_s} \frac{\partial f_s(\mathbf{w})}{\partial \mathbf{w}} \right] d^3 w \quad (31)$$

where $\mathbf{u} = \mathbf{v} - \mathbf{w}$ and \mathbf{I} is the identity matrix. S is the source of ions representing the ions generated from the neutrals of the beam. Because the collision operator conserves the number of particles, a loss-term S has to be included, otherwise, there could be no stationary solution to Eq.(30). The simplest particle loss-term is

$$L = -\frac{f_b}{\tau} \quad (32)$$

It corresponds to both particle and energy loss. With a τ independent of velocity, it constitutes a good representation of charge-exchange losses. A more sophisticated loss term distinguishing particle and energy loss is

$$L = -\frac{f_b}{\tau_p} + \frac{1}{v^2} \frac{\partial}{\partial v} \left[\left(\frac{1}{\tau_E} - \frac{1}{\tau_p} \right) \frac{v^3}{2} f_b \right] \quad (33)$$

where τ_E and τ_p , respectively energy and particle confinement times, can be functions of the velocity.

Solving Eq.(30) is a complex problem because it involves three-dimensional collision integrals that, even numerically, are heavy to evaluate¹⁶. In addition, this equation is non-linear because of the beam self-collision term $C(f_b, f_b)$. In order to simplify the problem one can assume (i) that self-collisions are negligible when the beam component is not a too large fraction of the plasma population (ii) that the beam distribution function is independent of the gyro-angle, (iii) that all background species are isotropic maxwellians. In this case, all the

collision integrals can be performed analytically and one arrives at the linear collision operator

$$C(f) = -\frac{1}{v^2} \frac{\partial}{\partial v} (\alpha(v)v^2 f) + \frac{1}{2v^2} \frac{\partial^2}{\partial v^2} (\beta(v)v^2 f) + \frac{1}{4v^2} \frac{\partial}{\partial \mu} \left[\gamma(v)(1-\mu^2) \frac{\partial f}{\partial \mu} \right] \quad (34)$$

expressed in terms of the particle velocity v and of the cosine of the pitch-angle $\mu = v_{||}/v$. α, β, γ are analytic expressions involving the error function¹⁷. These expressions can be further simplified by assuming, as was done above in the test-particle approach, that $V_{te} \gg v_b \gg V_{ti}$. One then arrives at the limits:

$$-\alpha v^2 + \frac{1}{2} \frac{\partial}{\partial v} (\beta v^2) = \frac{1}{\tau_s} (v^3 + v_c^3) \quad (35.1)$$

$$\beta = \frac{2T_e}{m_b \tau_s} \left(1 + \frac{v_\beta^3}{v^3} \right) \quad (35.2)$$

$$\gamma = \frac{v_\gamma^3}{\tau_s v} \quad (35.3)$$

where one recognises the above-defined slowing-down-time τ_s and the critical velocity v_c . The additional expressions for v_β and v_γ are¹⁷:

$$v_\beta^3 = \frac{3\sqrt{\pi}}{4} \left(\frac{2k_B T_e}{m_e} \right)^{1/2} \sum_i \frac{n_i}{n_e} Z_i^2 \frac{2k_B T_i}{m_i} \quad (36.1)$$

$$v_\gamma^3 = \frac{3\sqrt{\pi}}{4} \frac{m_e}{m_b} \left(\frac{2k_B T_e}{m_e} \right)^{3/2} \sum_i \frac{n_i}{n_e} Z_i^2 \quad (36.2)$$

Finally, retaining only the dominant terms one arrives at the standard form of the collision operator used for the investigation of fast-ions distribution functions:

$$C_1(f_b) = \frac{1}{\tau_s v^3} \left[v \frac{\partial}{\partial v} [(v^3 + v_c^3) f_b] \right] + Z_2 \frac{v_c^3}{2} \frac{\partial}{\partial \mu} \left[(1-\mu^2) \frac{\partial f_b}{\partial \mu} \right] \quad (37)$$

$$\text{with } Z_2 = \frac{\sum_i n_i Z_i^2 / m_b}{\sum_i n_i Z_i^2 / m_i} \quad (38)$$

It is amazing to note that while the original Landau form Eq.(31) and the linearised form for maxwellian background Eq.(34) conserve the number of particles, the collision operator Eq.(37) does not. Therefore the classical Fokker-Planck equation for fast-ions is written:

$$\frac{\partial f_b}{\partial t} = C_1(f_b) + S \quad (39)$$

without explicit loss term. The origin of the loss can be investigated by computing the evolution of the particle density

$$n_b = \int f_b d^3 v \quad (40)$$

for an isotropic distribution function $f_b(v)$ by integration of the above Eq.(39) in the absence of source

$$\frac{\partial n_b}{\partial t} = \frac{\partial}{\partial t} 2\pi \int_{-1}^1 d\mu \int_0^\infty v^2 f_b dv = -\frac{4\pi}{\tau_s} v_c^3 f_b(0) \quad (41)$$

implies that the origin of velocity space is a particle sink.

The equation (39) with $S=0$ is separable and the eigenfunctions of the pitch-angle operator [last term in Eq.(37)] are Legendre polynomials. Therefore an analytic solution of the stationary version of Eq.(39) can be obtained¹⁸ for a delta-function source

$$S(v, \mu) = \frac{S_0}{v^2} \delta(v - v_{b0}) \delta(\mu - \mu_{b0}) \quad (42)$$

where S_0 is the rate of injection of the beam particles. Note that the index “ $b0$ ” refers to the *initial* properties of the injected ions. The beam distribution function can be written:

$$f_b(v, \mu) = \frac{\tau_s S_0}{v^3 + v_c^3} \sum_{l=0}^{\infty} \frac{2l+1}{2} P_l(\mu_{b0}) P_l(\mu) \times \left[\frac{v^3}{v_{b0}^3} \frac{v_{b0}^3 + v_c^3}{v^3 + v_c^3} \right]^{(l+1)Z_2/6} \gamma(v_{b0} - v) \quad (43)$$

where γ is the step function. One notes that this distribution function is abruptly cut-off at the injection velocity $v=v_{b0}$. This results from the neglect of diffusion by thermal electrons, which, in reality, will accelerate some beam ions above the injection velocity. The characteristics of beam distribution functions have been illustrated by Van Eester¹⁹.

The beam distribution function takes a particularly simple form when the source is isotropic

$$S(v) = \frac{S_0}{v^2} \delta(v - v_0) \quad (44)$$

This is usually not very realistic for neutral beam injection¹⁹, unless the investigated properties of the beam distribution function are well represented by the first (isotropic) term of the series Eq.(43). However, it is quite appropriate for computing the distribution function of fusion-generated α -particles. For $\partial/\partial\mu=0$, Eq.(39) is particularly easy to solve and one obtains

$$f(v) = \frac{\tau_s S_0}{4\pi} \frac{1}{v^3 + v_c^3} \gamma(v_0 - v) \quad (45)$$

This is a good approximation of the α -particle distribution function and one should note that this function is very different from a maxwellian. At large velocity, it decays like $1/v^3$ rather than exponentially, and becomes flat below the critical velocity v_c .

In the general case of non-isotropic beam injection the beam component of the plasma will contribute to the parallel ($W_{//}$) and perpendicular (W_{\perp}) energy content of the plasma differently from the background species for which $W_{\perp}=2W_{//}$. This has an impact on the interpretation of the diamagnetic and equilibrium energy signals. At the lower densities the beam component can be an appreciable fraction of the total plasma energy content.

Similarly, in the reactor, the fast fusion products can contribute significantly to the total plasma beta.

IV. COMPARISONS WITH EXPERIMENTS

The experimental verification of the two basic processes of beam heating, namely ionisation and slowing-down, is not trivial because both processes depend on a number of plasma parameters and profiles. In all what precedes, we have considered the beam as a thin monoenergetic pencil of neutrals. This is not quite the case as the beam cross-section may be a substantial fraction of the poloidal cross-section of the plasma itself. Therefore, a realistic beam can be conceived as a number of parallel thin beamlets, each making its own path through the density, temperature and impurity concentration profiles. Ionisation is the easiest to check, by measuring the shine-through of the beam.

IV.A. Ionisation.

In the already quoted ITER work¹³, the theoretical increment in stopping cross-section, due to multi-step ionisation is compared with experimental results for both PNBI and NNBI in TFTR and JT-60, showing satisfactory agreement. Additional beam shine-through comparisons made in JT-60 can be found in Suzuki¹² and Oikawa⁷.

IV.B. Slowing down.

Obviously, checks of slowing-down are more indirect as the slowing down computation must start from the result of the ionisation computation, i.e. the beam-ion birth profile. For PNBI, the analysis of fast-ion tails is further complicated by the presence of half and third energy beam components (section II.A). On the experimental side, the direct measurement of fast ion distribution functions inside the plasma is presently not available. One can look at the distribution of the charge-exchange neutrals coming out of the plasma. However, this signal has a simple interpretation only in the case of rather small plasmas of low density, otherwise too few fast neutrals generated in the plasma bulk reach the plasma outside, all others being re-ionised. Comparisons based on charge-exchange spectra were made on PLT, showing good agreement between theory and experiment²⁰.

Another way of looking at tails is by measuring the neutron rate from D-D reactions (or from other fusion reactions if, e.g. DT if tritium is present). The fusion reaction rate is indeed very sensitive to tails as it peaks in the hundreds of keV range. It is however even more indirect than CX neutrals measurement as the deuterium

density and temperature profiles enter once more the computation of the reaction rate. After an abrupt switch-off of the NBI, the fast ion tail remains for a while, decaying with a one slowing-down time rate (appropriately averaged over the plasma volume). So does the neutron production rate. The decay rate of the fusion neutrons is thus an indirect measurement of the slowing-down time. Comparisons have been made in several machines^{20,21,6}, always giving good agreement with predictions.

An even more global way of making comparisons, which has become more or less standard, is to run a transport code equipped with a beam simulation package and to predict the total neutron flux from *beam-target* (the subject of the comparisons discussed just above), *beam-beam* and *thermal* fusion reactions and compare it with the experimentally measured flux²².

V. PHYSICS RESULTS WITH NBI

V.A. Heating.

NBI has been used in all major tokamaks in the world and has produced high temperature and high performance plasmas^{23,24}. Shots with NBI heating constitute a large fraction of the ITER database²⁵. NBI has also been used with success in DT experiments²⁶. Both D and T have been injected in a DT target plasma. The highest fusion power output (16.1 MW) shot in JET was obtained with 3.1 MW of ICRH power and 22.3 MW of beam power (with injection of 155 keV T and 80 keV D). It must be noted that most shots of this database are PNBI shots with a large fraction of the power coupled to bulk ions because of the relatively low injection energy. For a 1 MeV NNBI in ITER, the fraction coupled to ions will be smaller. One should note also that injection energies are often close to the optimum energy for the DT reaction. For example, for the record JET shot cited above, close to 40% of the reaction rate was due to beam-target reactions. This will no longer be the case in ITER.

V.B. Current Drive.

Efficient current drive has also been achieved with NBI¹. The recent results with NNBI on JT-60U are very promising in that they reflect a good understanding of the driven current deposition profile and a current drive efficiency somewhat higher than PNBI⁷.

V.C. Toroidal Rotation Drive.

When a fast ion is created in the plasma, it carries the toroidal angular momentum

$$L_T = m_b R v_{b0} \mathbf{e}_\phi = m_b R \mu v_{b0} = m_b R_T v_{b0} \quad (46)$$

where \mathbf{e}_ϕ is the unit vector in the toroidal direction, R is the birth radius of the ion R_T the tangency radius of the initial neutral (or of the beam pencil). The last equality in Eq.(44) simply results from the geometrical relation $R_T = \mu R$ and expresses the fact that the injected toroidal momentum is independent of the precise birth place of the ion along the neutral beam path. Once the neutral is ionised, the total angular momentum of the plasma has increased by the quantity Eq.(46). As shown experimentally in JET²⁷, this momentum will be transferred to the bulk plasma on three different time scales: (i) The ion that is born on a trapped trajectory, loses its momentum on a bounce time-scale. This momentum is transferred to the bulk plasma on the same time-scale by a $\mathbf{j} \times \mathbf{B}$ force due to the radial current associated with the displacement of the ion between its birth radius and the average radius of its banana orbit. (ii) The ion that is born on a passing trajectory will transfer its momentum by slowing down on the bulk plasma on a slowing down time scale. (iii) When the passing ion becomes part of the thermal population after full slowing down, it carries its residual toroidal momentum. The associated torques are balanced by toroidal momentum damping, which has been found to be anomalous. It is indeed much larger than the neoclassical estimates, and is usually close to the energy confinement time.

NBI can be used in ITER to induce toroidal rotation in addition to its obvious role of heating and current drive system. However, for high energy injection, the injected momentum per unit power ($\propto 1/v_b$) is much less than for present experiments with PNBI.

VI. FURTHER READING

A good introduction to Coulomb relaxation and to the analysis of beam heating of plasmas can be found in the book by Dnestrovskii & Kostamarov²⁸. Detailed analysis of Coulomb collisions can be found in the works by Sivukhin¹⁵ and Karney¹⁶. A technology-oriented description of NBI is given by Kunkel²⁹.

REFERENCES

1. D.W. FAULCONER, "Current Drive: NBI & RF", *These proc.*
2. P.N.YUSHMANOV et al., "Scalings for tokamak energy confinement", *Nucl. Fus.* **30**, 1999, (1990)
3. R. KOSLOWSKI, "Operational limits in tokamak machines and limiting instabilities", *These proc.*
4. R. KOCH & D. VAN EESTER, "Enhancement of reactivity by RF", *Plasma Phys. and Contr. Fus.* **35A**, A211 (1993), F. LOUCHE, R. KOCH, "Final Report on ITER subtask D350.1: Modelling of ICRH system heating performances with PION/PRETOR package", *LPP-ERM/KMS Brussels Report n°115* (1999)
5. K.H. BERKNER et al., "Intense, mixed-energy hydrogen beams for CTR injection", *Nucl. Fus.* **15**, 249, (1975)
6. K. USHIGUSA & JT-60 TEAM, "Steady state operation research in JT-60U", *Proc. 16-th IAEA Fus. Energy Conf., Montréal, IAEA Vienna*, Vol.1, 37, (1996)
7. T. OIKAWA, et al., "Heating and non-inductive current drive by negative-ion based NBI in JT-60U", *Proc. 17-th IAEA Fusion Energy Conference, Yokohama, IAEA Vienna*, paper IAEA-F1-CN-69/CD1/1 (1998)
8. J. PAMELA, "The physics of production, acceleration and neutralisation of large negative ion beams", *Plasma Phys. and Contr. Fusion*, **37**, 325 (1995)
9. A.C.RIVIERE, "Penetration of fast hydrogen atoms into a fusion reactor plasma", *Nucl. Fus.* **11**, 363, (1971)
10. D.R. SWEETMAN "Ignition condition in tokamak experiments and role of neutral injection heating", *Nucl. Fus.* **13**, 157, (1973)
11. R.K. JANEV et al., "Penetration of energetic neutral beams into fusion plasmas", *Nucl. Fus.* **29**, 2125, (1989)
12. S.SUZUKI et al. "Attenuation of high-energy neutral hydrogen beams in high-density plasmas", *Plasma Phys. Contr. Fus.*, **40**, 2097, (1998)
13. ITER team, et al., "ITER Physics basis", to be published in *Nucl. Fus.* (1999 or 2000)
14. J.G. CORDEY, "The neutral injection heating of toroidal plasmas to ignition", in *Physics of Plasmas Close to Thermonuclear Conditions*, EUR FU BRU/XII/476/80, Ed. CEC Brussels, **I**, 359 (1979).
15. D.V. SIVUKHIN, "Coulomb collisions in a fully ionized plasma" in *Reviews of Plasma Physics*, Ed. M.A. Leontovich, *Consultants Bureau New York* **4**, 93 (1966).
16. C.F.F. KARNEY, "Fokker-Planck and quasilinear codes", *Computer Physics Reports* **4**, 183 (1986).
17. D. ANDERSON, "Distortion of the distribution function of weakly RF heated minority ions in a tokamak plasma", *J. Plasma Phys.* **29**, 317 (1983)
18. J.D.Jr. GAFFEY, "Energetic ion distribution resulting from neutral beam injection in tokamaks", *J. Plasma Phys.* **16**, 149 (1976)
19. D. VAN EESTER, "Plasma heating and current drive: numerical methods", Second Carolus Magnus Summer School on Plasma Physics, Aachen 1995, *Transactions of Fusion Technology*, **29**(1996)258.
20. R.J. GOLDSTON, "Neutral beam injection experiments", *Physics of Plasmas Close to Thermonuclear Conditions*, EUR FU BRU/XII/476/80, Ed. CEC Brussels, **II**, 535 (1979).
21. W.W. HEIDBRINK et al., "Comparison of experimental and theoretical fast ion slowing down times in DIII-D", *Nucl. Fus.* **28**, 1897, (1988)
22. JET Team, "Fusion energy production from a deuterium-tritium plasma in the JET tokamak", *Nucl. Fus.* **32**, 187, (1992)
23. K. TOBITA, JT-60 Team, "Latest plasma performance and experiments on JT-60U", *Plasma Phys. and Contr. Fus.*, **41**(1999)A333.
24. E. THOMPSON, et al., "The use of neutral beam heating to produce high performance fusion plasmas, including the injection of tritium beams into the Joint European torus (JET)", *Phys. Fluids B.*, **5**(1993)2468.
25. K. THOMSEN et al., "ITER H mode confinement database update", *Nucl. Fus.* **34**, 131, (1994)
26. J. JACQUINOT, JET Team, "Deuterium-tritium operation in magnetic confinement experiments: results and underlying physics", *Plasma Phys. and Contr. Fus.*, **41**(1999)A13.
27. K. D. ZASTROW et al., "Transfer rates of toroidal angular momentum during neutral beam injection", *Nucl. Fus.* **38**, 257, (1998)
28. Y.N. DNESTROWSKII & D.P. KOSTAMAROV, "Numerical simulation of plasmas", Springer-Verlag (1986).
29. W.B. KUNKEL, "Neutral beam injection", in *Fusion* Ed. E. Teller, Academic press **1B** (1981).